Effects of molybdenum, silver dopants and a titanium substrate layer on copper film metallization

Y. K. KO, J. H. JANG, S. LEE, H. J. YANG, W. H. LEE*
School of Metallurgical and Materials Engineering, Kookmin University, Seoul 136-702, Korea

P. J. REUCROFT
Department of Chemical and Materials Engineering, University of Kentucky, Lexington, KY 40506, USA

J. G. LEE
School of Metallurgical and Materials Engineering, Kookmin University, Seoul 136-702, Korea
E-mail: lgab@kookmin.ac.kr

Annealing of 100 nm-thick Cu, Cu(Mo) and Cu(Ag) films was carried out to investigate the effect of dopant atoms on the films. Molybdenum (Mo) and silver (Ag) were selected as immiscible dopants for out-diffusion studies. A thermally grown SiO_2 layer and a sputtered Ti layer were used as substrates. The dopant and substrate effects were characterized in terms of surface morphology, resistivity, preferred orientation, and diffusional characteristics. The lowest observed resistivity was 2.32 $\mu\Omega \cdot$ cm in the Cu(Ag) film, which was lower than that in a pure Cu film of the same thickness. Ag addition enhanced the surface morphology and thermal stability of the Cu(Ag) films. The highest thermal stability was obtained in the case of a Cu(Mo)/Ti film which maintained film integrity to 800°C. A Ti substrate enhanced Cu(111) texture growth. A highly oriented Cu(111)-texture was obtained in the Cu(Mo)/Ti films. Cu diffusion through the Ti layer was limited in the (111)-textured Cu(Mo)/Ti films, which showed good potential as a diffusion barrier.
© 2003 Kluwer Academic Publishers

1. Introduction

Metallization in semiconductor devices has been developed to improve their performance and reliability. Multilevel interconnection is required for ULSI (ultra-large scale integrated-circuits) development as the feature size shrinks. The number of metal levels will continue to increase as the level of the circuit increases. The interconnect linewidth in the ULSI should also be decreased for complete integration. The narrow linewidth of metal interconnection lines results in higher current density and lower electromigration (EM) resistance. A new interconnection material is thus required for these demands.

Copper has received considerable attention as a potential interconnect material in advanced metallization technology since it possesses intrinsically better electromigration resistance and lower resistivity compared to aluminum [1–4]. However, Cu metallization has several important technical problems, such as passivation of the exposed Cu surface, adhesion of Cu to SiO_2, development of a Cu patterning process and surface roughness of the Cu film [5–7].

To address these problems, doping Cu with immiscible or soluble elements has been intensively studied in order to develop new interconnect materials in advanced metallization [8–13]. These alloying schemes are intended to dissociate the dopant out of the alloy film upon annealing, either in a vacuum or an oxygen atmosphere, in order to change the microstructure of the interconnects. Microstructural features of the metal interconnect affects its reliability and performance as the linewidth approaches 100 nm. A highly (111)-textured Al film had an excellent EM performance [14], and the Cu (111) structure is also expected to have good EM performance and reliability. In addition, the low resistivity of the metal increases device performance parameters, such as speed and also leads to a smaller RC time constant [1].

In this study, the Cu film thickness was about 100 nm. Mo and Ag were used as dopant atoms in the Cu films since they are immiscible in Cu at low temperatures. Mo and Ag are also slow and fast diffusing elements in Cu film, respectively. Dopant effects were characterized in terms of surface morphology, resistivity, texture

**Present Address*: Department of Advanced Materials Engineering, Sejong University, Seoul 143-747, Korea.

0022–2461 © *2003 Kluwer Academic Publishers*

and diffusional characteristics after annealing. Pure Cu films were also deposited to compare with the Cu alloy films. A Ti substrate layer was also employed to enhance the (111) texture of the Cu films.

2. Experimental

A (100) Si wafer was thermally oxidized to form a 10 nm SiO_2 layer. Cu(Mo) and Cu(Ag) alloy films having thickness of about 100 nm were deposited on the SiO_2 layer by direct current (DC) magnetron sputtering from Cu(5.0 at.% Mo) and Cu(3.0 at.% Ag) targets with a purity level of 99.999%, respectively. The Cu(Mo) and Cu(Ag) films were also deposited on a 10 nm Ti layer deposited on the SiO_2 by a sputtering method. In addition, unalloyed pure Cu film was also deposited for comparison. The sputtering conditions were as follows. The base pressure in the deposition chamber was 2×10^{-6} torr, the Ar pressure was 3 mTorr, the sputtering power was 180 W and the substrate temperature was ambient temperature. After deposition, Cu/SiO_2/Si, Cu/Ti/SiO_2/Si, Cu(Mo)/SiO_2/Si, Cu(Mo)/Ti/SiO_2/Si, Cu(Ag)/SiO_2/Si and Cu(Ag)/Ti/SiO_2/Si multilayer samples were vacuum annealed at a pressure of 1.5×10^{-6} torr for 30 minutes in the 300–800°C temperature range.

Film thickness was measured by a surface profilometer. After annealing, the resistivity as a function of annealing temperature was measured by the four-point probe method. An x-ray diffractometer (XRD) was employed to identify phases in the Cu films and obtain crystallographic texture information. Depth profiling using Auger electron spectroscopy (AES) was carried out to investigate diffusional characteristics of the chemical elements in the films. Surface morphology of the films was observed by field emission scanning electron microscopy (FESEM).

3. Results and discussion

Vacuum annealing was carried out to investigate the effect of Mo and Ag dopants on surface morphology of 100 nm-thick Cu films. The surface morphologies of the pure Cu, Cu(Mo) and Cu(Ag) films annealed at 600°C and 700°C are shown in Fig. 1. Fig. 1a and b

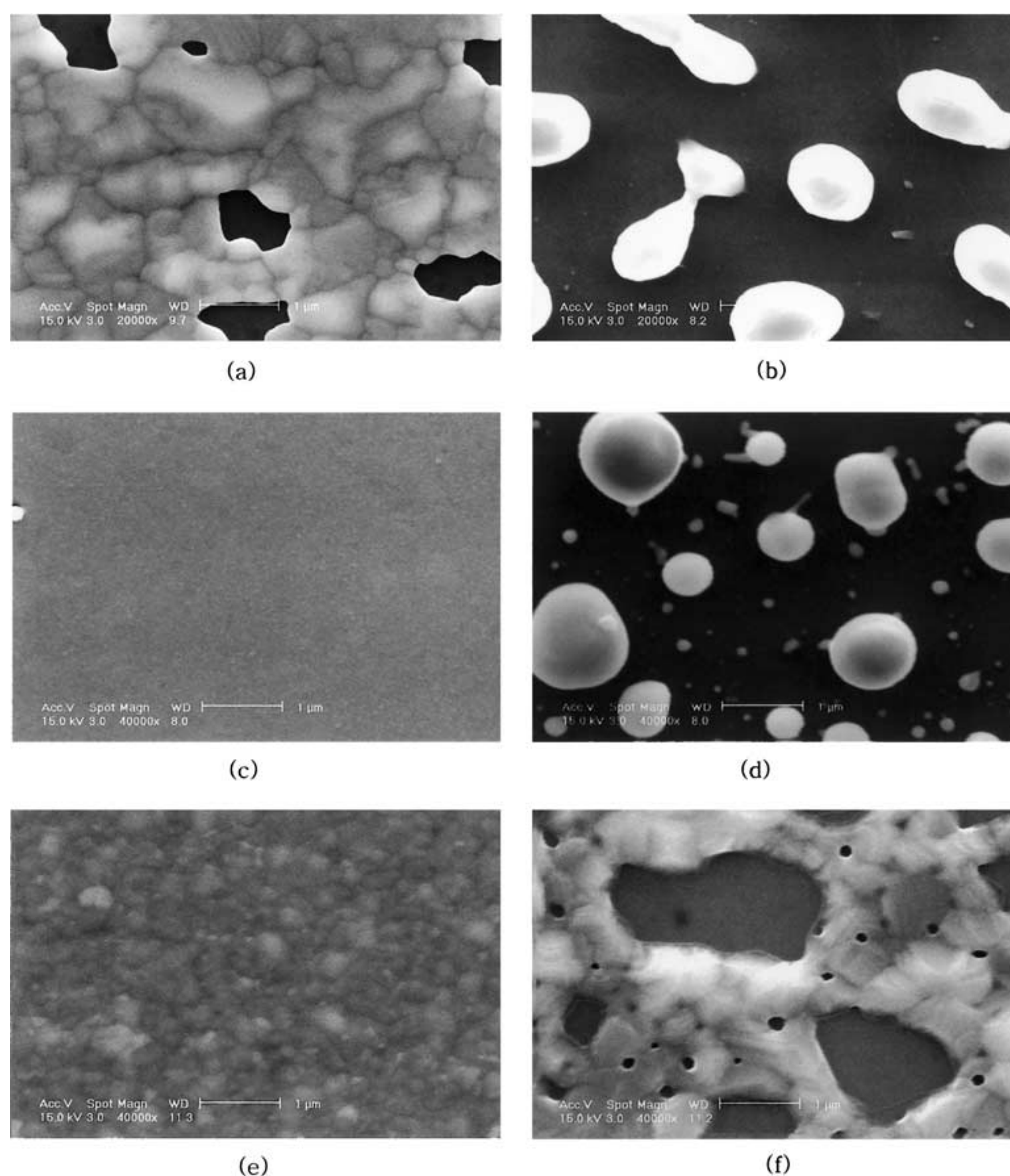

Figure 1 FESEM micrographs of pure Cu films annealed at (a) 600°C and (b) 700°C, Cu(Mo) films annealed at (c) 600°C and (d) 700°C, and Cu(Ag) films annealed at (e) 600°C and (f) 700°C. Film thickness was 100 nm.

shows SEM micrographs of the 100 nm pure Cu films annealed at 600°C and 700°C, respectively. A big hole was formed in the film annealed at 600°C and Cu agglomeration occurred at 700°C. Alloying effects of Mo and Ag enhanced the thermal stability of the Cu films to 600°C as shown in Fig. 1c and e, respectively. However, the Cu(Mo) film was completely agglomerated, and the Cu(Ag) film formed big holes at an annealing temperature of 700°C, as shown in Fig. 1d and f, respectively.

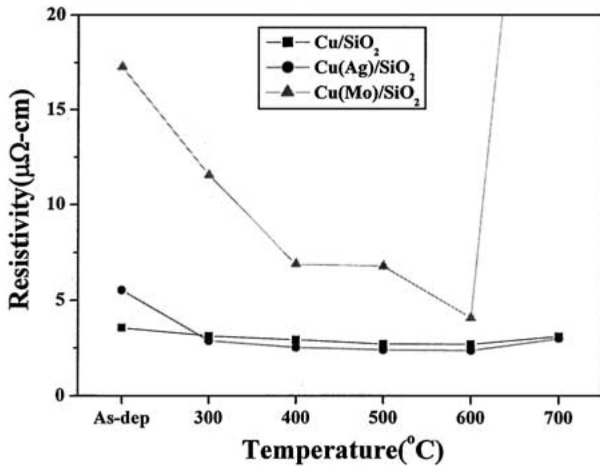

Figure 2 Resistivity of 100 nm-thick pure Cu, Cu(Ag) and Cu(Mo) films as a function of annealing temperature.

Mo and Ag atoms are larger in size than a Cu atom. This size difference induces stress around the solute atoms in the Cu solid solution. The stress field and grain boundaries interfere with electron flow and result in an increased resistivity of the Cu(Mo) and Cu(Ag) films in the as-deposited condition, as shown in Fig. 2. Fig. 2 shows the resistivity of Cu films that are about 100 nm in thickness. The resistivities of the Cu(Mo) and the Cu(Ag) films were systematically decreased with increased annealing temperature. The resistivity decrease is attributed to stress relaxation and grain growth [15]. The resistivity of the Cu(Mo) films did not decrease below that of pure Cu film at any temperature and reached a very high value at 700°C due to Cu agglomeration. However, the resistivity of the Cu(Ag) film, annealed at 300°C and above, decreased below that of the pure Cu film. The minimum observed resistivity was 2.32 $\mu\Omega \cdot$ cm obtained from the Cu(Ag) films annealed at 500°C and 600°C. The fast diffusing Ag atoms in the Cu(Ag) films resulted in a low resistivity in comparison to the Cu(Mo) films where a slower diffusing Mo atom resulted in a high resistivity.

Diffusion of Ag and Mo atoms in the Cu films was investigated with Auger depth profile studies and the results are shown in Fig. 3. Most of the Ag atoms in the Cu(Ag) film appeared to out-diffuse to the free surface and the substrate interface after annealing at 500°C, as shown in Fig. 3a. In contrast, Mo atoms in the Cu(Mo)

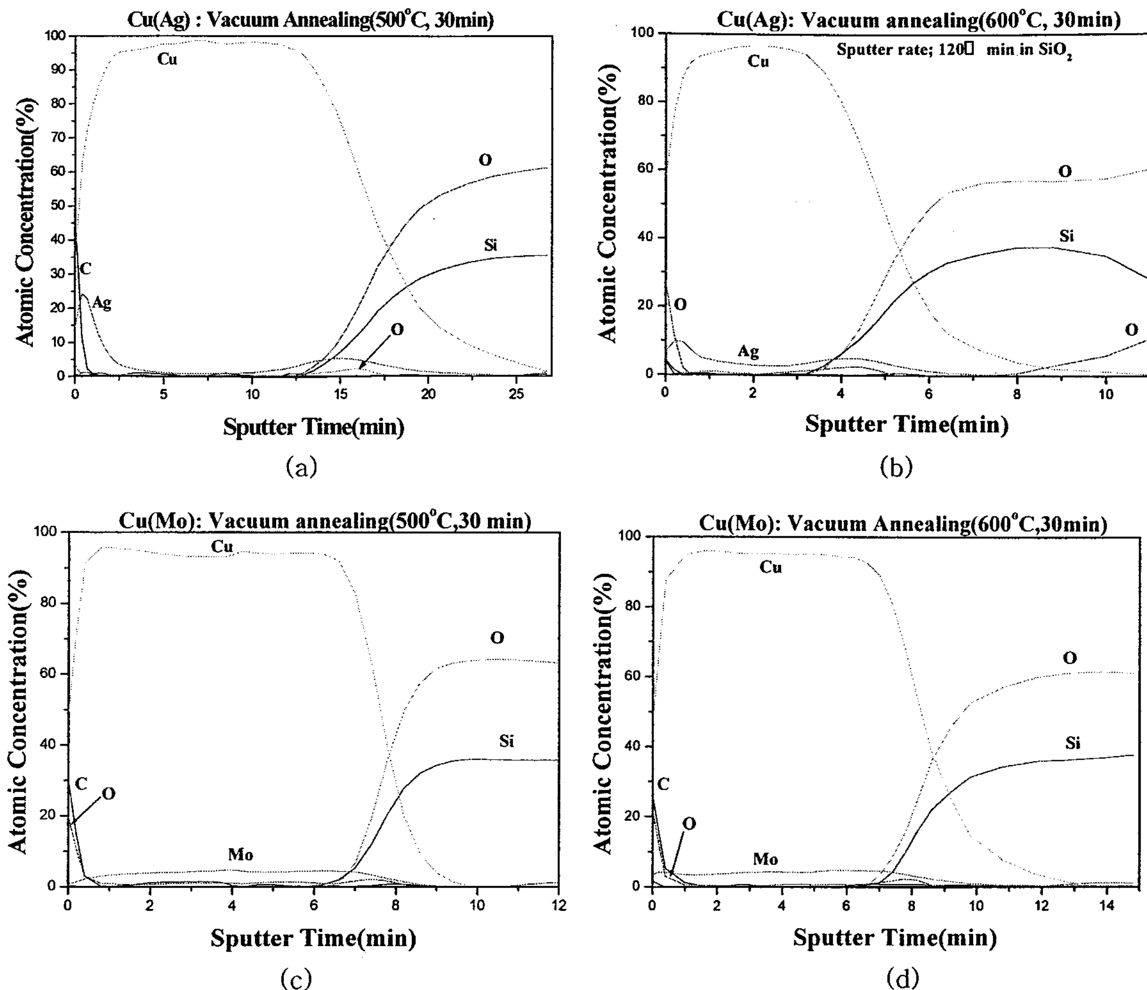

Figure 3 AES depth profiles of Cu(Ag) films vacuum-annealed at (a) 500°C and (b) 600°C, and Cu(Mo) films vacuum-annealed at (c) 500°C and (d) 600°C for 30 minutes. Film thickness was 100 nm.

film did not significantly migrate toward the surface and the interface, and are almost uniformly distributed throughout the film annealed at 500°C, as shown in Fig. 3c. The high resistivity of the Cu(Mo) film annealed at 500°C resulted from reduced grain growth and low Mo diffusion as shown in Figs 1c and 3c. The degree of Ag out-diffusion was lower in the Cu(Ag) film annealed at 600°C since Ag solubility in the Cu film is higher at 600°C than that at 500°C. Whereas, out-diffusion of Mo atoms was enhanced in the Cu(Mo) film annealed at 600°C compared to the film at 500°C, as shown in Fig. 3c and d.

XRD patterns of the pure Cu, Cu(Mo) and Cu(Ag) films are shown in Fig. 4. XRD patterns of the pure Cu films showed Cu(111) and (200) peaks in the as-deposited condition. The intensity ratio of Cu(111) to (200) peaks was about 2 showing a random orientation of Cu grains, as shown in Fig. 4a. The peak ratio was not much changed in the pure Cu films annealed at 300°C and 700°C. A Cu(111) texture was developed in the Cu(Mo) and Cu(Ag) films in the as-deposited condition, as shown in Fig. 4b and c, respectively. The driving force of the (111)-texture growth in the films is considered to be interface energy minimization [16]. Mo and Ag atoms in the Cu film produced an increased

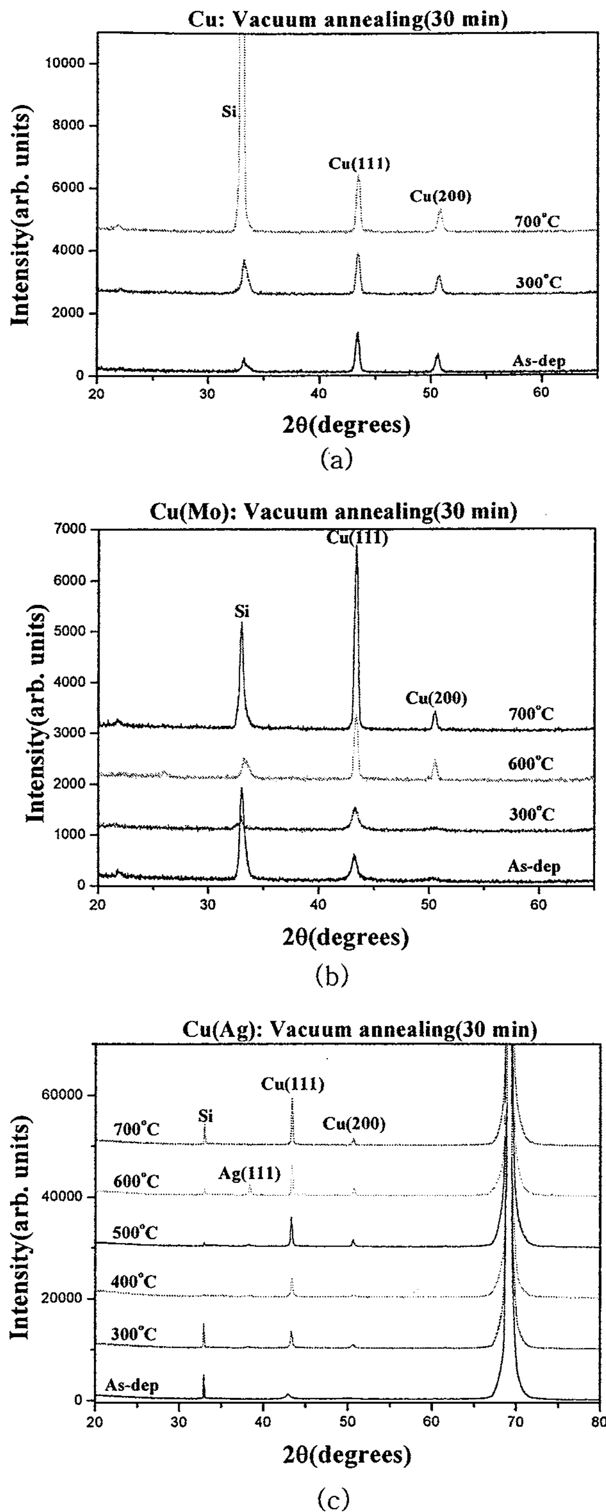

Figure 4 XRD patterns at various annealing temperatures for 100 nm-thick (a) pure Cu, (b) Cu(Mo) and (c) Cu(Ag) films.

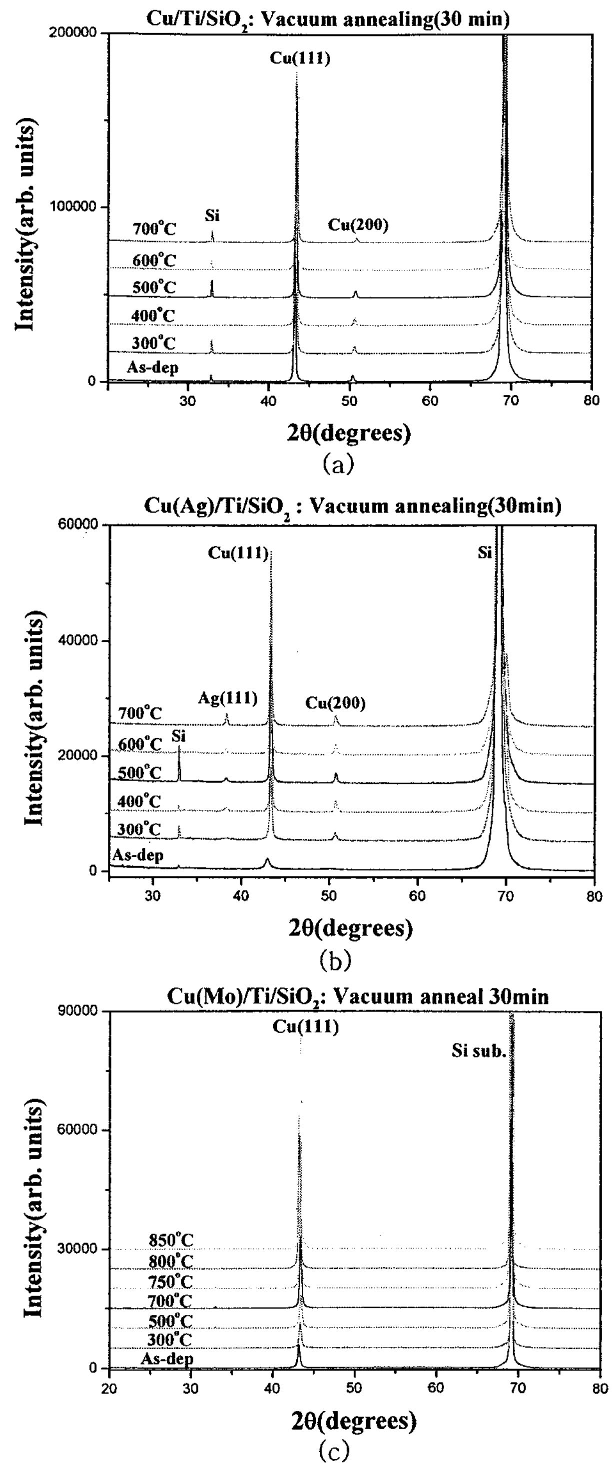

Figure 5 XRD patterns at various annealing temperature for 100 nm-thick (a) Cu/Ti, (b) Cu(Ag)/Ti and (c) Cu(Mo)/Ti films.

interface energy during deposition of the Cu(Mo) and Cu(Ag) films. The Cu(111) texture was then evolved to decrease the interface energy in the films. The Cu(200) peaks were evolved in the Cu(Mo) and Cu(Ag) films annealed at 600°C and 300°C, respectively, as shown in Fig. 4b and c. Strain energy minimization is considered to be the driving force of the (200) peak evolution [16]. The Cu (200) peak evolution in the films was attributed to Mo and Ag diffusion, as shown in Fig. 3. The Mo and Ag diffusions could not maintain a compacted (111) structure and produced strain energy, since they had different atomic sizes compared to the Cu atom, and also created vacancies by inter-diffusion.

A Ti layer under the pure Cu and the Cu(Ag) films decreased the Cu(200) peak intensity. The Cu(200) peaks disappeared entirely in the Cu(Mo)/Ti film, as shown in Fig. 5. The Cu(111) structure evolution was enhanced on the Ti film in the as-deposited condition since an amorphous alloy is formed at the interface between Cu and Ti [17].

The amorphous alloy at the interface thus contributed to the decreased lattice mismatch between Cu and Ti and led to a decreased internal stress at the interface. This interaction at the interface can lead to (111) texture evolution by an interface energy minimization process. The Cu(Mo)/Ti film showed a highly oriented (111) structure. The (111) texture is important in determining the reliability of the Cu interconnects [18–20]. AES depth profiles of the Cu(Mo)/Ti and Cu(Ag)/Ti films annealed at 600°C are shown in Fig. 6. Ti was out-diffused from the interface to the free surface of both films. Ag atoms in the Cu(Ag)/Ti film were also out-diffused to the free surface in the Cu(Ag) film as shown in Fig. 6a. The fast diffusing Ag atoms could lead to local strain energy formation around vacancies. The strain in the film could then result in Cu(200) peak evolution by strain energy minimization. In contrast, the Mo concentration was not significantly changed in the Cu (Mo) film, which is expected to be in a

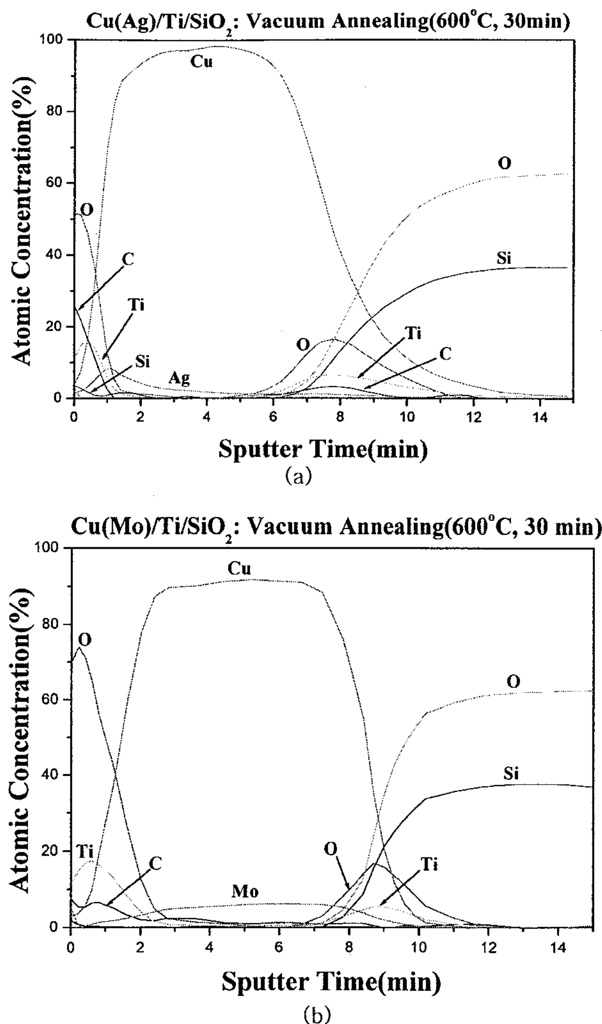

Figure 6 AES depth profiles of a 100 nm-thick Cu(Ag)/Ti film vacuum-annealed at (a) 600°C and a 100 nm-thick Cu(Mo)/Ti film vacuum-annealed at (b) 600°C for 30 minutes.

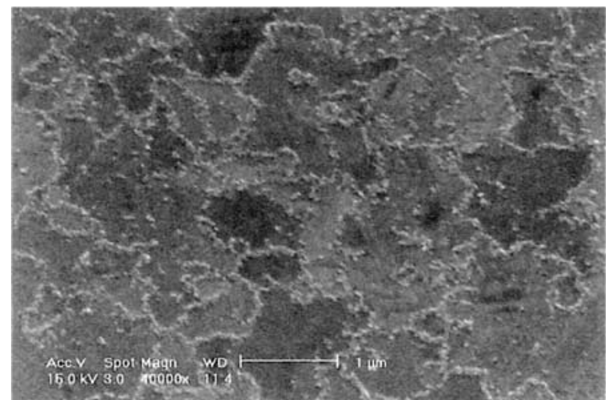

(a)

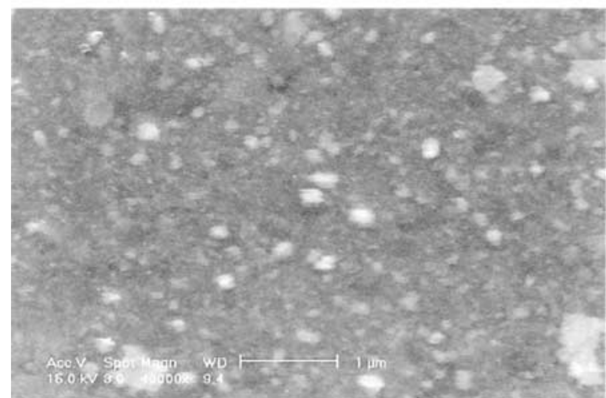

(b)

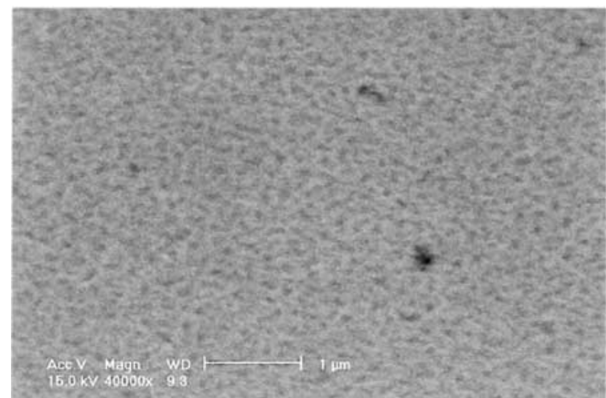

(c)

Figure 7 FESEM images of a 100 nm-thick Cu/Ti film annealed in vacuum at (a) 700°C, a 100 nm-thick Cu(Ag)/Ti film annealed in vacuum at (b) 700°C, and a 100 nm-thick Cu(Mo)/Ti film vacuum-annealed at 800°C for 30 minutes.

low strain energy state during the annealing, as shown in Fig. 6b. The perfectly oriented (111) structure of Cu(Mo) film was thus formed by slow diffusion of Mo atoms and by low lattice mismatch of the amorphous alloy with Cu at the interface. The low lattice mismatch induces low stress at the interface, which can then lead to Cu(111) texture growth. The dense Cu(111) structure in Cu(Mo)/Ti films shows limited diffusion of Cu through the Ti under-layer compared to the Cu(111) and Cu(100) structures in the Cu(Ag)/Ti films, as shown in Fig. 6a and b.

The Ti under-layer also increased thermal stability of the pure Cu, Cu(Mo) and Cu(Ag) films, as shown in Fig. 7. Fig. 7a shows the pure Cu/Ti film annealed at 700°C, indicating the enhanced thermal stability of the film compared to the pure Cu film shown in Fig. 1b. The enhanced stability is attributed to increased adhesion from amorphous alloy formation at the interface between Cu and Ti, and from strong-bond formation [21] at the interface between the Ti under-layer and the SiO_2 substrate.

The thermal stability of the Cu(Ag)/Ti film was also increased in comparison to the Cu(Ag) film annealed at 700°C, as shown in Figs 7b and 1f, respectively. The Cu(Mo)/Ti film showed even more enhanced thermal stability at 800°C compared to the Cu(Mo) film at 700°C, as shown in Figs 7c and 1d, respectively. The enhanced stability of the Cu(Ag)/Ti and Cu(Mo)/Ti films was attributed to the strength of the alloy films in addition to adhesion strength at the interfaces.

4. Conclusions

Cu(Ag) films, containing about 3 at.% of Ag, systematically decreased resistivity on annealing and reached a minimum resistivity of 2.32 $\mu\Omega \cdot$cm, which is a lower resistivity than that of pure Cu films of the same thickness. Surface morphology and thermal stability of the Cu films were also enhanced by Ag addition. The stability was increased even more, especially in Cu(Mo)/Ti film, by utilizing a Ti under-layer. The Ti substrate enhanced Cu(111) texture growth. A perfectly oriented Cu(111) texture was obtained in the Cu(Mo)/Ti films. Cu diffusion through the Ti layer was limited in the Cu(Mo)/Ti film, which shows excellent potential as a Cu diffusion barrier.

Acknowledgments

This work was supported by Grant No. 1999-1-30100-002-5 from the Basic Research Program of the Korea Science & Engineering Foundation.

References

1. S. P. MURARKA, R. J. GUTMANN, A. E. KALOYEROS and W. A. LANFORD, *Thin Solid Films* **236** (1993) 257.
2. A. JIAN, T. T. KODAS, R. JAIRATH and M. J. HAMPDEN-SMITH, *J. Vac. Sci. Technol.* B **11** (1993) 2107.
3. S. P. MURARKA and S. W. HYMES, *Solid State Mater. Sci.* **20** (1995) 87.
4. Y. J. PARK, V. K. ANDLEIGH and C. V. THOMPSON, *J. Appl. Phys.* **85** (1999) 3546.
5. R. LIU, C. S. PAI and E. MARTINEZ, *Solid State Electron.* **43** (1999) 1003.
6. X. W. LIN and D. PRAMANLK, *ibid.* **41** (1998) 63.
7. W. A. LANFORD, P. J. DING, W. WANG, S. HYMES and S. P. MURARKA, *Mater. Chem. Phys.* **41** (1995) 192.
8. P. J. DING, W. WANG, W. A. LANFORD, S. HYMES and S. P. MURARKA, *Appl. Phys. Lett.* **65** (1994) 1778.
9. H. ITO, Y. NAKASAKI, G. MINAMIHABA, K. SUGURO and H. OKANO, *Appl. Phys. Lett.* **63** (1993) 934.
10. J. LI, J. W. MAYER and E. G. COLOGAN, *J. Appl. Phys.* **70** (1991) 2820.
11. W. H. LEE, H. Y. CHO, B. S. CHO, J. Y. KIM, Y.-S. KIM, W.-G. JUNG, H. KWON, J. H. LEE, C. M. LEE, P. J. REUCROFT and J. G. LEE, *J. Vac. Sci. Technol.* A **18** (2000) 2972.
12. *Idem.*, *J. Electrochem. Soc.* **147** (2000) 3066.
13. W. H. LEE, H. Y. CHO, B. S. CHO, J. Y. KIM, Y.-S. KIM, W.-G. JUNG, H. KWON, J. H. LEE, C. M. LEE, P. J. REUCROFT, E. G. LEE and J. G. LEE, *Appl. Phys. Lett.* **77** (2000) 2192.
14. K. HASHIMOTO and H. ONODA, *ibid.* **10** (1989) 120.
15. K. BARMAK, G. A. LUCADAMO, C. CABRAL JR., C. LAVOIE and J. M. E. HARPER, *J. Appl. Phys.* **87** (2000) 2204.
16. C. V. THOMPSON and R. CAREL, *Mater. Sci. Eng.* B **32** (1995) 211.
17. J. GENG, A. SCHÜLER, P. REINKE and P. OELHAFEN, *J. Appl. Phys.* **84**(5) (1998) 2876.
18. S. VAIDYA and A. K. SINHA, *Thin Solid Films* **75** (1981) 253.
19. D. B. KNORR, D. P. TRACY and K. P. RODBELL, *Appl. Phys. Lett.* **59** (1991) 3241.
20. D. B. KNORR and K. P. RODBELL, *J. Appl. Phys.* **79** (1996) 2409.
21. T. OHWAKI, K. AOKI, T. YOSHIDA, S. HASHIMOTO, Y. MITSUSHIMA and Y. TAGA, *Surface Science* **433–435** (1999) 496.

Received 10 May
and accepted 24 September 2002